ResearchGate

See discussions, stats, and author profiles for this publication at: https://www.researchgate.net/publication/318968375

NbN superconducting nanonetwork fabricated using porous silicon templates and high-resolution electron beam...

Article *in* Nanotechnology · August 2017

DOI: 10.1088/1361-6528/aa8479

CITATIONS
0

READS
18

8 authors, including:

M. Salvato
University of Rome Tor Vergata
105 PUBLICATIONS **699** CITATIONS
SEE PROFILE

S. L. Prischepa
Belarusian State University of Informatics an...
168 PUBLICATIONS **764** CITATIONS
SEE PROFILE

Vitaly Bondarenko
Belarusian State University of Informatics an...
162 PUBLICATIONS **1,011** CITATIONS
SEE PROFILE

Carmine Attanasio
Università degli Studi di Salerno
191 PUBLICATIONS **1,104** CITATIONS
SEE PROFILE

Библиотека БГУИР

All content following this page was uploaded by Carmine Attanasio on 20 October 2017.

The user has requested enhancement of the downloaded file.

PAPER

NbN superconducting nanonetwork fabricated using porous silicon templates and high-resolution electron beam lithography

To cite this article: M Salvato *et al* 2017 *Nanotechnology* **28** 465301

View the article online for updates and enhancements.

Библиотека БГУИР

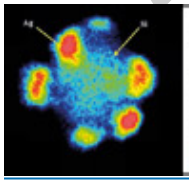
Discover Nanoparticle Solutions
for Exploratory Research
Find out more at AVS International Symposium
Florida, USA - booth 601
NanoGen
Nanocluster Sources

MANTIS

This content was downloaded from IP address 150.146.205.185 on 20/10/2017 at 14:20

IOP Publishing Nanotechnology
Nanotechnology 28 (2017) 465301 (6pp) https://doi.org/10.1088/1361-6528/aa8479

NbN superconducting nanonetwork fabricated using porous silicon templates and high-resolution electron beam lithography

M Salvato[1], R Baghdadi[2], C Cirillo[3], S L Prischepa[4,5], A L Dolgiy[4], V P Bondarenko[4], F Lombardi[2] and C Attanasio[3]

[1] Dipartimento di Fisica, Università di Roma 'Tor Vergata', I-00133, Rome and CNR-SPIN Salerno, via Giovanni Paolo II 132, I-84084 Fisciano (Sa), Italy
[2] Quantum Device Physics Laboratory, Department of Microtechnology and Nanoscience, Chalmers University of Technology, SE-41296 Göteborg, Sweden
[3] CNR-SPIN Salerno and Dipartimento di Fisica 'E. R. Caianiello', Università degli Studi di Salerno, via Giovanni Paolo II 132, I-84084 Fisciano (Sa), Italy
[4] Belarusian State University of Informatics and Radioelectronics, P. Brovka 6, Minsk 220013, Belarus
[5] National Research Nuclear University 'MEPHI', Kashirskoe Highway 31, Moscow 115409, Russia

E-mail: attanasio@sa.infn.it

Received 4 May 2017, revised 25 July 2017
Accepted for publication 7 August 2017
Published 20 October 2017

Abstract

Superconducting NbN nanonetworks with a very small number of interconnected nanowires, with diameter of the order of 4 nm, are fabricated combining a bottom-up (use of porous silicon nanotemplates) with a top-down technique (high-resolution electron beam lithography). The method is easy to control and allows the fabrication of devices, on a robust support, with electrical properties close to a one-dimensional superconductor that can be used fruitfully for novel applications.

Keywords: porous silicon, electron beam lithography, one-dimensional superconductivity, quantum phase slips

(Some figures may appear in colour only in the online journal)

1. Introduction

The synthesis of nanostructures based on robust self-assembled nanoporous templates recently received a growth of interest. This bottom-up technique allows one to fabricate, with high reproducibility, a large number of nanostructures in a single-step process [1–4]. In particular, the deposition of ultrathin films of superconducting materials on templates, both porous alumina and porous silicon (PS), as well as on inorganic membranes, gives the possibility of creating interconnected nanowire networks where commensurability effects [5–7], or properties typical of a single superconducting nanowire are observed [8–10]. What essentially happens is that, due to the very reduced film thickness, the deposited material tends to fill only the substrate pitch, so as to obtain structures which resemble a network of interconnected wires. In these systems the average width, w, can be assumed to be equal to the periodic pore spacing, a, minus the pore diameter, ϕ, (figures 1(a) and (b)): $w = a - \phi$. Furthermore, if w is of the order of the coherence length of the superconducting material, ξ, each nanowire in the network behaves as a one-dimensional (1D) superconductor [11].

Nowadays, superconducting nanowires (SNWs) are attracting great interest because of their promising use in superconducting-based nanoelectronics. SNWs are considered as accessible candidates for current standards [12], SQUID-like sensors [13, 14], microwave and photon detectors [15, 16], quantum-computing circuits [17–19] and also as

Библиотека БГУИР

 © 2017 IOP Publishing Ltd Printed in the UK

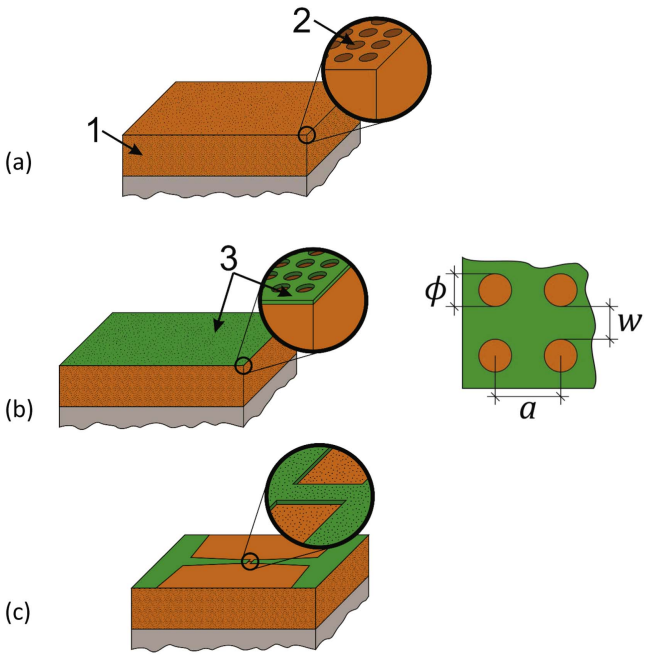

Figure 1. Schematic representation of the (a) PS layer formation. 1—porous layer 1.5 μm thick. 2—porous surface; (b) deposition of the NbN ultrathin film. 3—the film inherits the porous structure of the PS template: ϕ is the pore diameter, a is the center-to-center pore distance, and $w = a - \phi$ is the width of the superconducting channels; (c) fabrication of the NbN nanoporous nanostrip by EBL. Porous media are primed by the resist.

1D interconnects in complex nanodevices [20]. Very recently, a superconducting nonvolatile memory device based on loops made from superconducting nanowires was proposed [21]. The large potential for application of SNWs comes from the proved duality between these 1D systems and the Josephson Junctions, which are the basic units of most of the superconducting nanoelectronics [12]. The duality comes from the presence of phase fluctuations (known as phase slips) of the order parameter inside a homogeneous 1D SNW [11, 12]. When phase slip phenomena are present, the superconducting order parameter is locally depressed and superconductivity disappears. As a result, a finite electrical resistance is observed well below the bulk superconducting critical temperature, T_c, in the case of thermally activated phase slips (TAPS) [22, 23] and down to $T = 0$ in the case of quantum phase slips (QPS) [24–27]. In principle, this dissipation limits the use of superconducting nanodevices. It is therefore crucial the study of superconductivity in 1D systems. However, it is not an easy task to fabricate a single 1D nanowire for superconductors like NbN with a few nanometers coherence length, since nanometer scale dimensions cannot be obtained with the usual lithographic techniques. For this reason alternative approaches were very recently developed to overcome this difficulty [28–30].

Concerning the materials choice, it is worth noticing that the investigated SNW networks in literature are largely Nb-based [5–7, 9, 10] while most of the superconducting devices, such as Josephson junctions and radiation detectors, are typically produced in Nb or NbN technology [31]. In particular, nanowire arrays in superconducting nanowire single photon detectors are mainly based on NbN [16]. Moreover, the investigation of NbN nanowire networks on porous templates could be useful to determine the possible application of the SNW networks as radiation detectors. In particular, NbN is a dirty superconductor characterized by a short ξ, high resistivity in the normal state, ρ, and high critical temperature, T_c [32, 33]. The small value of ξ (of the order of 3–4 nm) makes it possible to successfully fabricate, on porous templates, superconducting nanowire networks with the effective diameter, $d_{\mathrm{eff}} \approx \sqrt{t \cdot w}$, smaller than 5 nm (here t is the film thickness) that are not dominated by thermal fluctuations [11]. The high value of the resistivity also enhances the probability amplitude to have QPS in 1D superconductors [11, 34]. Finally, even at these extreme conditions the value of T_c can be higher than 10 K [32, 33].

In this work, we combine the bottom-up template technique with a top-down approach to obtain a superconducting NbN interconnected network. The top-down method is based on high-resolution electron beam lithography (EBL) which allows the fabrication of structures with lateral dimensions as small as 10 nm [35–38]. The combination of the two techniques makes it possible to ultimately fabricate, on a robust support, a network containing a very small number ($N = 6$) of superconducting nanowires (figure 1(c)). The process is undoubtedly quicker and much easier to control with respect to the most recent attempts reported in the literature [28–30]. Furthermore, it paves the way to create a structure containing only one nanowire, if self-assembled templates with pores with the appropriate values of a and ϕ are used. These structures can be valuably used in the field of the superconducting electronics [12–21].

2. Experimental methods

The PS templates were fabricated by an electrochemical anodic etching of p-type monocrystalline Si wafers. The thickness of the anodized silicon layer was $\sim$1.5 μm and the average center-to-center distance was $a = 2\phi$ so that $w = \phi$. Three different PS templates were used; they differ in the values of the average diameters of the pores, $\phi = 5$, 7.5 and 10 nm so that in all the cases $w \sim \xi$. They will be referred to as PS5, PS7, and PS10, respectively. Figure 2(a) shows a scanning electron microscope (SEM) image of the PS10 surface. The average diameter of the pores, measured by statistical analysis in different areas of the micrograph, agrees with the nominal value $\phi = 10$ nm [39].

NbN ultrathin films were deposited by magnetron sputtering using an Ar flow rate of 60 sccm and an N_2 flow rate of 6.5 sccm. The base pressure inside the deposition chamber was 1×10^{-8} Torr and the mixture pressure during the deposition was 3.2×10^{-3} Torr. The deposition rates were determined by measuring d_{NbN} of films deposited on Si/SiO_2 substrates partially shadowed by a mechanical mask and kept at a fixed temperature T_s. The obtained values were 0.41 nm/s and 0.27 nm/s at $T_s = 300$ °C and $T_s = 500$ °C, respectively. Different NbN thicknesses, of the order of ξ, were studied and their surface morphology was analysed by SEM. The

Buonomera BYMP

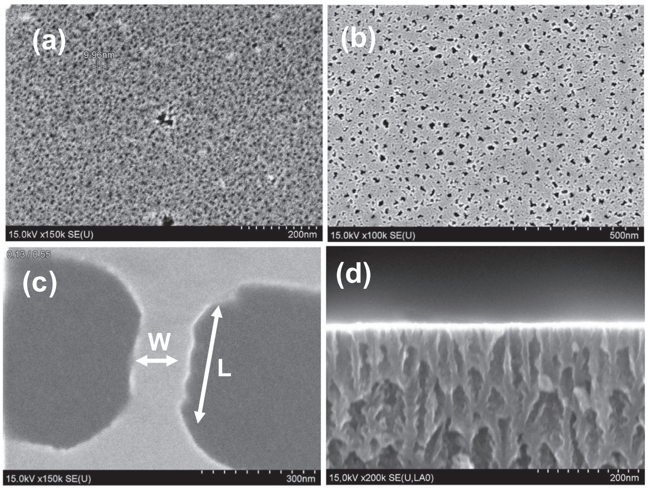

Figure 2. SEM image of the surface of the (a) PS10 template; (b) sample PS10-3.7; (c) NbN nanostrip with width $W = 65$ nm and length $L = 270$ nm fabricated on the sample PS10-3.7. (d) Cross section SEM image of the sample PS10-3.7 after the EBL process.

fabricated samples were indexed by the substrate name followed by a number indicating the NbN layer thickness, d_{NbN}, expressed in nanometers. For example, PS5-5.6 indicates the sample obtained by sputtering 5.6 nm of NbN on the PS5 substrate. Figure 2(b) shows a SEM pattern of the PS10-3.7 sample deposited by keeping the substrate temperature during the deposition at $T_s = 300$ °C. The presence of the pores is still evident confirming that the porous structure is maintained after the NbN deposition.

Samples were then patterned by high-resolution EBL in strips with width, W, in the range of 60–320 nm and length, L, in the range of 270–1370 nm. A single mask process with a negative resist (ma-N 2403) was used. It was spanned on the sample surface at 6000 rpm for one minute ($\sim$180 nm thick) and then was heated on a contact hot-plate at 95 °C for one minute. A direct e-beam writing was performed using the e-beam lithography system (100 kV, JEOL JBX-9300FS) to define the desired geometries. The resist was exposed using a 1 nA e-beam current, with a dose of 220 $\mu C/cm^2$, and then developed with MF-CD-26 for 45 seconds and finally rinsed with deionized water and dried with nitrogen. The unmasked NbN was etched in a reactive-ion etching (RIE) system by NF_3 gas for 16 seconds (flow = 50 sccm; radio frequency power = 50 W). A laser interferometer end-point detection was used to stop the etching process. Finally, the resist was removed by placing the chip on the heated Microposit mR-400 held at 65 °C. Different values of W were considered in order to obtain SNW networks with different values of N along the direction of the flowing current ($N \sim W/2\phi$ (see schematics in figure 1(b))). For example, the strip with $W = 60$ nm processed on the PS5-3.7 sample consists of $N \sim 60/10 = 6$ SNWs. Figure 2(c) shows the SEM image of a strip with $W = 65$ nm and $L = 270$ nm. The presence of the pores was confirmed by the SEM cross-section image of the sample PS10-3.7 taken after the EBL procedure, as shown in figure 2(d). It is evident that the porous structure is maintained up to the surface of the substrate.

To obtain SNW networks on porous substrates one needs to deposit continuum percolative paths between the pores without filling them. The achievement of this condition depends on both the thickness of the superconducting layer and the substrate temperature, T_s. In particular, a thick NbN layer will unavoidably fill the pores covering the whole substrate surface. Moreover, for large values of d_{NbN} one expects that the pores will play the role of defects positioned below the NbN layer with the result of depressing the superconducting properties. On the contrary, small d_{NbN} will cause a lack of the coalescence process favouring the formation of unconnected grains along the percolative paths. A high value of T_s would enhance the diffusion of the deposited species that consequently would not be confined between the pores. Therefore, to select the optimal value for d_{NbN}, several NbN ultrathin films with varying thicknesses were deposited on PS templates in different conditions. For the thickest analysed samples, $d_{NbN} = 7.2$ nm, deposited at $T_s = 300$ °C on the PS5, PS7, and PS10 templates the value of T_c (defined as the temperature at which $R = 0.5R_N$, where R_N is the normal state resistance just before the transition to the superconducting state) increases with decreasing ϕ. This result suggests that in this case the thick NbN layer covers the whole surface of the templates including the pores which now behave as defects. In fact, when the size of the defects becomes smaller (which happens decreasing the value of ϕ coming from PS10 to PS5), an increase of 0.4 K in T_c is measured. On the contrary, for the thinnest samples the resistive curves show that only the sample PS10-2.7 has a complete superconducting transition. The sample PS7-2.7 does not reach the zero-resistance state completely, while the sample PS5-2.7 has an insulating behavior. These results can be interpreted considering that for such a thin NbN layer a full percolative superconducting path is created only on the PS10 template, which is characterized by the largest w. Differing from the previous case, T_c decreases as a function of w as expected when the size of the superconducting sample is reduced [40]. In the intermediate case, $d_{NbN} = 3.7$ nm, again T_c decreases as a function of w. For this NbN thickness the pores are still not filled and the species effectively grows on the border between the pores, the percolative paths between the voltage contacts are formed and the SNW network is achieved in all the templates. Finally, the effect of the substrate temperature on the NbN growth was analysed by depositing the NbN films of $d_{NbN} = 3.7$ nm keeping the substrate at $T_s = 500$ °C. In this case the critical temperature does not appreciably change when the NbN is deposited on the PS5, PS7 and PS10 templates. Furthermore, the value of T_c is the same of the film deposited on a flat Si/SiO_2 substrate. What happens is that the higher mobility of the species on the substrate, enhanced by the high value of T_s, probably causes shorts across the pores so that the SNW network is not formed any more. Summarizing, by measuring the values of T_c, we found that the best growth conditions, to obtain continuous percolative paths along the channels, were realized when a NbN 3.7 nm thick film was deposited at $T_s = 300$ °C. In

Библиотека БГУИР

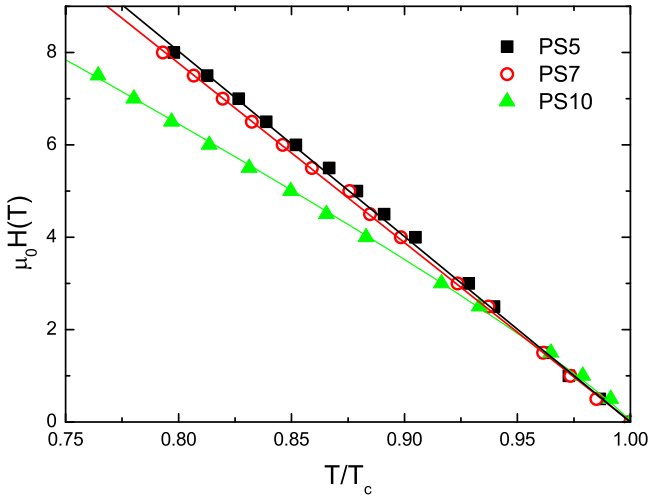

Figure 3. H_{c2} as a function of the reduced temperature of the SNW network 3.7 nm thick obtained on the PS5, PS7, and PS10 templates. Solid lines are a guide to the eye.

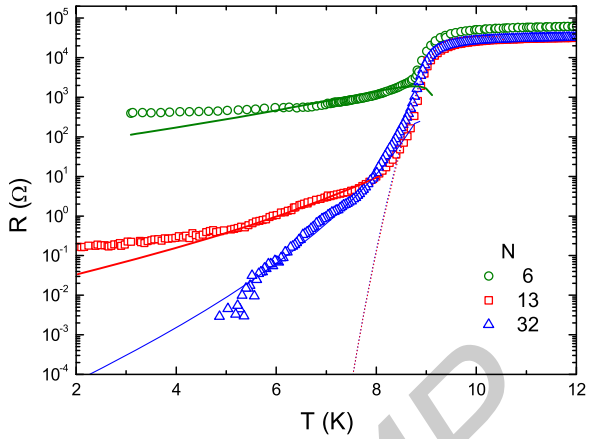

Figure 4. Resistive transitions of the PS5-3.7 bridges with different number of SNWs, N. The dashed lines (thick solid) are the results of the fitting procedure obtained by considering the TAPS (QPS) process. The fitting parameters are reported in table 1.

particular, we present here a detailed analysis of sample PS5-3.7 where, because of the small value of w, 1D superconductivity can be more easily established ($d_{\mathrm{NbN}} \sim w \sim \xi$).

The resistivity ρ of SNW networks cannot be easily evaluated due to the particular nanowires arrangement [9, 10]. However, by measuring the $H_{c2}(T)$ phase diagram (the magnetic field has been always applied perpendicularly to the plane of the substrate) it is possible to estimate the diffusivity, $D = 1.097/(-\mu_0 dH_{c2}/dT)|_{T=T_c}$ [32, 33], and the zero-temperature superconducting coherence length, $\xi(0)$, of the samples. In figure 3 the upper perpendicular critical fields of the SNW network 3.7 nm thick obtained on the PS5, PS7, and PS10 templates are plotted as a function of the reduced temperature, T/T_c. For the sample PS5-3.7, we get $D = 0.19$ cm^2/s. Taking an electron scattering time $\tau \approx 3 \times 10^{-15}$ s, valid for NbN nanowires [32, 33], one obtains for the electron mean free path $\ell = \sqrt{3D\tau} \approx 0.5$ nm. Moreover, knowing that for NbN $\rho\ell \approx 10^{-5}\mu\Omega \cdot \mathrm{cm}^2$ [32, 33], we can estimate for the low-temperature resistivity a value of 200 $\mu\Omega \cdot$ cm. Assuming the linear behavior of the temperature dependence of perpendicular upper critical field, it is also possible to evaluate the superconducting coherence length, since $\mu_0 H_{c2}(0) = \Phi/2\pi\xi^2(0)$, where Φ is the magnetic flux quantum [41]. This relation gives $\xi(0) = 2.91$ nm which also implies that the sample is in the dirty limit.

3. Discussion

Here we investigate the evolution of the superconducting state in the PS5-3.7 sample after it was patterned in strips of different widths by an EBL process. The data shown in figure 4 refer to three different strips with $W = 65$ nm, 130 nm and 320 nm each having a number of SNWs equal to $N = 6$, 13 and 32, respectively. All the structures have a well-defined $T_c^{\mathrm{onset}} \approx 9$ K (taken as the temperature at which $R = 0.9R_N$) only one degree lower with respect to the value measured for the unpatterned samples, which confirms that a percolative path is preserved along the whole strips and that superconductivity is achieved. The curves have different shapes indicating that different mechanisms are established at low temperatures. For $N = 32$, the resistance changes of seven order of magnitudes below T_c^{onset} reaching a value which is zero in the limit of the sensitivity of our experimental set-up. On the other hand, when the value of N is reduced, a finite value of the resistance is measured down to the lowest measured temperature ($T \sim 2$ K). In the case of $N = 6$ the resistance is three orders of magnitude larger with respect to the sample with $N = 13$.

To better investigate the physics at play, the experimental results were analysed in the framework of the theoretical models proposed for 1D superconductors of length Λ in the presence of TAPS and QPS processes. In the case of thermal fluctuations, the data were fitted by using the expression [42]

$$R_{\mathrm{TAPS}} \sim R_Q \frac{\Lambda}{\xi(T)} \frac{T_c}{T} \sqrt{\frac{U(T)}{k_B T}} \exp\left(-\frac{U(T)}{k_B T}\right) \qquad (1)$$

where $U(T) = U(0)(1 - T/T_c)^{3/2}$ is the phase slip activation energy and $\xi(T) = \xi(0)\sqrt{1 - T/T_c}$. Here $U(0) \approx 0.83(S/\xi(0))(R_Q/\rho)k_B T_c$ [43], where $S = t \cdot w$ and $R_Q = h/4e^2 = 6.45$ kΩ is the quantum resistance.

In the case of quantum fluctuations phenomena one gets [43, 44]

$$R_{\mathrm{QPS}}(T) = \frac{h\Gamma_{\mathrm{QPS}}}{2eI} \qquad (2)$$

where

$$\Gamma_{\mathrm{QPS}} = \frac{S_{\mathrm{QPS}}}{\tau_0} \frac{\Lambda}{\xi(T)} \exp(-S_{\mathrm{QPS}}). \qquad (3)$$

Библиотека БГУИР

Table 1. Sample parameters obtained to reproduce the $R(T)$ curves of the PS5-3.7 bridge with different N. See the text for details.

Sample (N)	Λ(nm) (from both equations (1) and (2))	$U(0)$ (meV)	A
32	34	3.6	11
13	64	3.4	3.5
6	66	—	4

Here Γ_{QPS} is the QPS activation rate, $\tau_0 \approx h/\Delta$ is the characteristic time of the superconductor and $S_{QPS} = A\left(\frac{R_Q}{R_N}\right)\left(\frac{\Lambda}{\xi(T)}\right)$ is the QPS action, with A a numerical constant of the order of the unity. Within this theoretical framework the only free parameters are Λ and $U(0)$ for TAPS and Λ and A for QPS. The best fitting curves that reproduce the data of the samples with $N = 32$ and $N = 13$ are obtained considering both the TAPS (dashed lines, equation (1)) and the QPS (thick solid lines, equation (2)) contributions in the high- and in the low-temperature regions, respectively. However, for $N = 6$ the reduction of the number of interconnected wires results in the pronounced resistance tail in the whole measurement region which was reproduced by equation (2) only. Overall, the fits are fairly good, especially if one considers that equations (1) and (2) were derived for single nanowires, while here we are dealing with arrays with undefined lengths, finite widths and activation energies distribution. The values of the parameters extracted from the fitting procedure are reported in table 1. For the samples with $N = 32$ and $N = 13$ the same value of Λ was extracted by both equations (1) and (2). Our results show the effect of TAPS and QPS inside networks of NbN SNWs whose size and thickness are of the same order of the superconducting coherence length. This confirms the 1D character of the units which form our structures. The evolution from TAPS to QPS with the reduction of N is a strong indication that isolated 1D SNWs, obtained by further reducing W, are governed by quantum effects. On the other hand, the increase of N, even preserving quantum behavior, favours the emergence of thermal effects which become dominant when a large number of SNWs are connected together to form the network. For each SNW, the width w represents an average value that, on long distances and for large strip areas, can vary considerably. When the width W of the strips obtained by the EBL process is larger, the probability of obtaining percolative paths with w wider than the given nominal value increases and this suppresses QPS in favour of TAPS. From the fitting procedure one has that the values of Λ are consistent with this scenario, since the increase in the distribution of widths w can on average reduce the length over which the fluctuations occur. Analogously, the values of A scale with N, which indicates that the QPS rate increases, decreasing N. Finally, the values obtained for the activation energy are comparable with the ones reported for Nb nanowire arrays deposited on PS [45].

4. Conclusions

In summary, we have shown that, combining a bottom-up technique, obtained by using PS templates, with a top-down process, defined using a high-resolution EBL, it is possible to fabricate a superconducting network consisting of a very small number of NbN nanowires. The analysed system presents a suppression of the superconductivity at low temperatures due to the phase fluctuations of the order parameter. The main advantage of the proposed method is that it allows the creation, in an easy way, of a quasi-1D superconductor with an effective diameter of the order of few nm that can be fruitfully used in superconducting nanodevices.

Acknowledgments

M S was partially supported by NanoSC-COST action MP1201. A L D acknowledges the partial financial support from the Belarusian Foundation for Fundamental Research, grant T16M-012.

ORCID iDs

C Attanasio https://orcid.org/0000-0002-3848-9169

References

[1] Rabin O, Hertz P R, Lin Y-M, Akinwande A I, Cronin S B and Dresselhaus M S 2003 *Adv. Funct. Mater.* **13** 631
[2] Hallet X, Mátéfi-Tempfli M, Michotte S, Piraux L, Vanacken J, Moshchalkov V V and Mátéfi-Tempfli S 2009 *Small* **5** 2413
[3] Koblischka M R, Zeng X L and Hartmann U 2016 *Phys. Status Solidi* A **213** 1069
[4] Trezza M, Cirillo C, Dolgiy A L, Redko S V, Bondarenko V P, Andreyenka A V, Danilyuk A L, Prischepa S L and Attanasio C 2016 *Supercond. Sci. Technol.* **29** 015011
[5] Welp U, Xiao Z L, Jiang J S, Vlasko-Vlasov V K, Bader S D, Crabtree G W, Liang J, Chik H and Xu J M 2002 *Phys. Rev.* B **66** 212507
[6] Vinckx W, Vanacken J, Moshchalkov V V, Mátéfi-Tempfli S, Mátéfi-Tempfli M, Michotte S and Piraux L 2006 *Eur. Phys. J.* B **53** 199
[7] Trezza M, Cirillo C, Prischepa S L and Attanasio C 2009 *Europhys. Lett.* **88** 57006
[8] Luo Q, Zeng X Q, Miszczak M E, Xiao Z L, Pearson J, Xu T and Kwok W K 2012 *Phys. Rev.* B **85** 174513
[9] Cirillo C, Trezza M, Chiarella F, Vecchione A, Bondarenko V P, Prischepa S L and Attanasio C 2012 *Appl. Phys. Lett.* **101** 172601
[10] Trezza M, Cirillo C, Sabatino P, Carapella G, Prischepa S L and Attanasio C 2013 *Appl. Phys. Lett.* **103** 252601
[11] Arutyunov K Y, Golubev D S and Zaikin A D 2008 *Phys. Rep.* **464** 1
[12] Mooij J E and Nazarov Y V 2006 *Nature Phys.* **2** 169
[13] Hopkins D S, Pekker D, Goldbart P M and Bezryadin A 2005 *Science* **308** 1762
[14] Johansson A, Sambandamurthy G, Shahar D, Jacobson N and Tenne R 2005 *Phys. Rev. Lett.* **95** 116805

Библиотека БГУИР

[15] Webster C H, Fenton J C, Hongisto T T, Giblin P, Zorin A B and Warburton P A 2013 *Phys. Rev.* B **87** 144510
[16] Natarajan C M, Tanner M G and Hadfield R H 2013 *Supercond. Sci. Technol.* **25** 063001
[17] Mooij J E and Harmans C J P M 2005 *New J. Phys.* **7** 219
[18] Ku J, Manucharyan V and Bezryadin A 2005 *Phys. Rev.* B **82** 134518
[19] Astafiev O V, Ioffe L B, Kafanov S, Pashkin Y A, Arutyunov K Y, Shahar D, Cohen O and Tsai J S 2012 *Nature* **484** 355
[20] Hor Y S, Welp U, Ito Y, Xiao Z L, Patel U, Mitchell J F, Kwok W K and Crabtree G W 2005 *Appl. Phys. Lett.* **87** 142506
[21] Murphy A, Averin D V and Bezryadin A 2017 *New J. Phys.* **19** 063015
[22] Rogachev A and Bezryadin A 2003 *Appl. Phys. Lett.* **83** 512
[23] Rogachev A, Bollinger A T and Bezryadin A 2005 *Phys. Rev. Lett.* **94** 017004
[24] Giordano N 1988 *Phys. Rev. Lett.* **61** 2137
[25] Bezryadin A, Lau C N and Tinkham M 2000 *Nature* **404** 971
[26] Lau C N, Markovic N, Bockrath M, Bezryadin A and Tinkham M 2001 *Phys. Rev. Lett.* **87** 217003
[27] Zgirski M, Riikonen K-P, Touboltsev V and Arutyunov K Y 2008 *Phys. Rev.* B **77** 054508
[28] Bezryadin A and Goldbart P M 2010 *Adv. Mater.* **22** 1111
[29] Morgan-Wall T, Hughes H J, Hartman N, McQueen T M and Markovic N 2014 *Appl. Phys. Lett.* **104** 173101
[30] Baumans X D A *et al* 2016 *Nat. Commun.* **7** 10560
[31] Seidel P 2015 *Applied Superconductivity: Handbook on Devices and Applications* (Weinheim: Wiley-VCH)
[32] Chockalingam S P, Chand M, Jesudasan J, Tripathi V and Raychaudhuri P 2008 *Phys. Rev.* B **77** 214503
[33] Semenov A *et al* 2009 *Phys. Rev.* B **80** 054510
[34] Masuda K, Moriyama S, Morita Y, Komatsu K, Takagi T, Hashimoto T, Miki N, Tanabe T and Maki H 2016 *Appl. Phys. Lett.* **108** 222601
[35] van der Zant H S J, Webster M N, Romijn J and Mooij J E 1994 *Phys Rev.* B **50** 340
[36] Bartolf H, Engel A, Schilling A, Il'in K, Siegel M, Hübers H-W and Semenov A 2010 *Phys. Rev.* B **81** 024502
[37] Delacour C, Pannetier B, Villegier J-C and Bouchiat V 2012 *Nano Lett.* **12** 3501
[38] Baghdadi R, Arpaia R, Charpentier S, Golubev D, Bauch T and Lombardi F 2015 *Phys. Rev. Applied* **4** 014422
[39] Trezza M *et al* 2008 *J. Appl. Phys* **104** 083917
[40] Marsili F, Gaggero A, Li L H, Surrente A, Leoni R, Lévy F and Fiore A 2009 *Supercond. Sci. Technol.* **22** 095013
[41] Tinkham M 1996 *Introduction to Superconductivity* (Singapore: McGraw-Hill)
[42] Golubev D S and Zaikin A D 2008 *Phys. Rev.* B **78** 144502
[43] Bae M H, Dinsmore R C III, Aref T, Brenner M and Bezryadin A 2009 *Nano Lett.* **9** 1889
[44] Golubev D S and Zaikin A D 2001 *Phys. Rev.* B **64** 014504
[45] Cirillo C, Prischepa S L, Trezza M, Bondarenko V P and Attanasio C 2014 *Nanotechnology* **25** 425205

Библиотека ВГУР

View publication stats